ARTICLE NO. 79-0671R

C80-110

Twin-Jet Shielding

S. P. Parthasarathy,* R. F. Cuffel,* and P. F. Massier†
Jet Propulsion Laboratory, California Institute of Technology, Pasadena, Calif.

For an over/under-the-wing engine configuration on an airplane, the noise produced by the upper jet flow is partially reflected by the lower jet. An analysis has been performed which can be used to predict the distribution of perceived noise levels (PNL) along the ground plane at takeoff for an airplane which is designed to take advantage of the over/under shielding concept. Typical contours of PNL, the shielding benefit in the shadow zone, and the effective perceived noise levels (EPNL) values at 3.5 n. mi. from brake release as well as EPNL values at sideline at 0.35 n. mi. have been calculated. This has been done for a range of flow parameters characteristic of engines producing inverted velocity profile jets suitable for use in a supersonic cruise vehicle. Reductions up to 6.0 EPNdB in community noise levels can be realized when the over engines are operated at higher thrust and the lower engines simultaneously operated with reduced thrust keeping the total thrust constant. A noise reduction on the sideline also would occur if the spanwise distance between the engines is small enough for shielding in this direction to be beneficial.

Nomenclature

b = distance, [see Eq. (33)]
C = see Fig. 5
c = speed of sound
D = diameter of jet
F = jet thrust
H = view factor
k = wave number
l = eddy length
$\dot{m}$ = mass flow rate
M = Mach number
N = noisy jet
n = number of eddies
O = brake release point
p = sound pressure
P = any point on the ground plane
Q = quiet jet
r = radius
R = distance [see Eq. (2) and Fig. 4]
S = distance between jets, midpoint of the exit plane of the two nozzles (see Figs. 1 and 4).
T = transmission coefficient
U = velocity, ripple velocity
u' = amplitude of eddy velocity
V = jet velocity
W = distance [see Eq. (3) and Fig. 4]
x = distance from brake release on the ground plane
X,Y,Z = coordinates (see Fig. 4)
α = angle between jet axis and horizontal equal to the sum of the slope of the flight path and the inclination of the engine axis to the flight path. It is not the angle of attack. (see Fig. 4)
β = angle [see Eq. (4) and Fig. 4]
δ = ratio r_i/r_0
Δ = difference symbol
ϵ = angle [see Eq. (14) and Figs. 2 and 7]
θ = angle (see Fig. 4)
λ = wavelength
ρ = density
ϕ = angle in the cross-sectional plane of the jets

Subscripts and Superscripts

f = effect of flight
i = referred to inlet; also "inner"
j = jet
mix = mixed condition
0 = see Fig. 4
o = outer
p = condition at peak power of sound radiated
R = reference value
s = surroundings
T = total
$'$ = particular coordinate system (see Fig. 4)

Presented as Paper 79-0671 at the AIAA 5th Aeroacoustics Conference, Seattle, Wash., March 12-14, 1979; submitted April 13, 1979; revision received Jan. 28, 1980.

Index categories: Aeroacoustics; Noise.

*Member of the Technical Staff. Member AIAA.
†Group Supervisor. Associate Fellow AIAA.

I. Introduction

It is known that quiet jets can hide noisy ones when two or more are located in close proximity of each other. The sound of the noisy jet is intercepted by the quieter jet and is redirected with the result that a beneficial noise reduction occurs in the line of sight, provided the quieter jet is located between the noisy one and the observer. Since commercial airplanes generally have multiple engines, a reorientation of these engines to achieve benefits from fluid shielding may, in certain instances, be possible. Aircraft with over/under-the-wing engine arrangements, for example, produce several effective perceived noise decibels (EPNdB) less noise below the aircraft than when all engines are installed under the wing. Even more suppression may be possible when the thrust of the upper engine is higher than that of the lower. The objective of this study was to evaluate the perceived noise levels (PNL) radiated from a configuration of two engines in close proximity. The engines are considered to be mounted vertically in line and each jet consists of coaxial flows in which the velocity profiles are inverted. It will be shown in a later section how additional shielding benefits arise when the spanwise separation of the two over/under pairs on either side of the aircraft is comparatively small. When the spanwise separation is large, the resulting intensities of noise on the ground are obtained by doubling the values obtained for a single pair of over/under engines.

Experimental investigations of twin-jet shielding have been performed by Bhat[1] and Kantola.[2] Bhat showed that the noise in the downstream direction at 120-160 deg from the inlet depends very strongly only on that part of the velocity profile which the observer can "see" directly. In these directions, a quiet jet can hide a noisy one. Near 90 deg to the inlet, the noise depends mainly on the peak jet velocity. A quiet jet is not able to hide a noisy jet here, indicating that the noise penetrates the near-jet flow. Kantola[2] investigated both

twin-round and twin-rectangular jets at typical jet engine conditions at various nozzle-to-nozzle spacings. It was shown that the layer of cooler ambient air which separates the hot high-velocity streams produces the discontinuities at which sound waves undergo reflection and refraction. In the downstream directions, total internal reflection at the boundary of the near jet causes a complete masking of the noise from the far jet.

Noise reduction in the region where the sound from the upper jet is intercepted by the lower jet may be attributed to two mechanisms, viz., turbulent scattering[3] and total reflection[4] of sound at the boundaries of the lower jet where an abrupt change in conditions and properties (velocity and speed of sound) of the medium occurs. Sound waves at high frequencies are well-scattered by turbulence and this is expected to be the dominant mechanism when the sound readily penetrates the lower jet. This occurs at flow speeds below the ambient speed of sound. However, for high-temperature, high-speed jet flows characteristic of flows produced by engines for future supersonic aircraft, reflection is expected to be the dominant mechanism of noise reduction in the shielding zone. In this case, most of the sound of high-intensity propagating downstream at acute angles with respect to the upper jet are totally reflected by the lower jet flow.[4] Scattering could still be important for those weak sound waves propagating at angles between 90 and 180 deg with respect to the jet axis, i.e., in the forward quadrant.

In the shielded zone, it has been found that the noise reduction begins at a certain frequency and increases rapidly (logarithmically) to a constant value with increasing frequency.[2] This relatively abrupt onset of shielding, i.e., a noise reduction $\geq$ 3 dB, is such that the wavelength λ_0 at the onset of shielding is approximately 1.4 times the distance S between the two jets. The distance S is also the diameter of the jets at the merging point. The constant value of λ_0/S occurs over a range of values of S/D from 1.3 to 5 in the experiments of Kantola and is independent of flow velocities and temperatures. A linear relationship between λ_0 and the size of the jet, which is an obstacle for the passage of sound, is characteristic of diffraction. Long waves creep around obstacles and therefore do not contribute to noise reduction. Short waves, which are either reflected by the jet or scattered in their passage through the jet, are responsible for the shielding. The region over which shielding occurs is referred to as the shadow. The shadow in turn consists of the narrow umbra and the wider penumbra regions. As the spacing between the jets increases, the shadows will be narrower and the noise levels lower. This means that shielding improves with larger jet separations. When the jets are near each other, however, the shadow is wider and this may be a more desirable condition in the vicinity of airports. In addition, other favorable effects due to jet interaction, viz., more rapid jet spreading and correspondingly more rapid noise reduction at the source might result. This does happen, as exhibited by the data obtained by Kantola,[2] where values of PNL greater than 3 dB were observed for jets of equal thrust.

II. Analytical Model

In the following shielding analysis of two separated jets it is assumed that the thickness of the jet shear layer is much smaller than the wavelength of sound, which in turn is much smaller than the jet circumference. When the wavelength is equal to or larger than twice the jet circumference, there is no shielding. It should be noted that the wavelength at the peak power of the sound radiated by a round jet occurs at a Strouhal number of about 0.3, i.e.,

$$(f_p D/U_j) = (C/\lambda_p)(D/U_j) = 0.3$$

where

$$\lambda_p = (D/0.3M_j) = (\pi D/0.94M_j)$$

For high-speed jets of Mach no. $M_j \sim 2$-3, λ_p is approximately equal to one-half to one-third of the circumference of the jet. Sound of this wavelength therefore is also shielded. The major contribution to the PNL occurs from wavelengths shorter than λ_p, which is a fortunate circumstance, because in the calculations to follow, it will be assumed that all wavelengths are shielded without serious error. In addition, coaxial jets with inverted profiles exhibit an inherent suppression of long wavelength noise (which cannot be shielded) with the result that the contribution of these long wavelengths to PNL is even smaller.

The assumption that the shear layers are thin is met in practice. In actual fact, the jet shear layers do have a sharp interface and a highly corrugated boundary and are difficult to treat exactly. But as the sample data show, the shielding effects seem to be explainable in these simple terms. It is assumed that the noise sources are incoherent and sound pressures add as mean squares. In the analysis, the shielding jet is treated as a simplified smooth slug flow, the intensity in the shadow is calculated, and to this the noise due to the quiet shielding jet is added to determine the final sound pressure. To begin with, the equation for plane waves at plane boundaries is used. The eddy Mach waves, which dominate in the case of supersonic jets, are sound waves emanating from the region of their origin. These waves have conical fronts and are highly directional. For such waves, the simplified shielding calculations may give adequate results.

Eddy Mach waves are not the only source of noise however. There is also the noise which originates in the subsonic parts of the flow, and is less directional. There is also noise caused by shock waves which interact with eddies. All of these noise sources and their locations and directivities need to be given as inputs for the shielding calculation. Jet instabilities induced by slight circumferential nonuniformities of flow, as well as other instabilities sometimes enhanced by flight velocity, etc., may need to be considered differently. In fact, if large oscillations occur, such as those seen in both screeching and crackling jets, modeling the shielding by a smooth slug flow may be inadequate.

For the present calculations, information on source distribution, the merging distance, etc., are unavailable. In this model, the upper jet is simply treated as a point source with the same directivity as observed in the far field. The model will be adequate, except when the two jets are so close that they merge within a short distance, thereby exposing only a small part of the sources in the shear layers. As mentioned previously, the long wavelength sources which do not contribute much to the PNL may not be shielded, but the error in assuming that all sources are located at a point may not be significant. Also, the intended use of shielding is to expose all

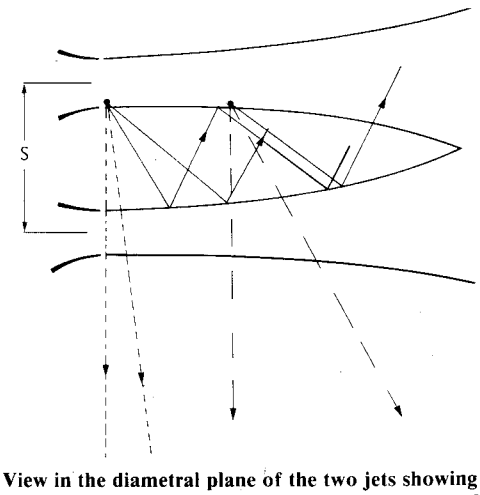

Fig. 1 View in the diametral plane of the two jets showing the shear layer boundaries and rays undergoing partial, total, and multiple reflections.

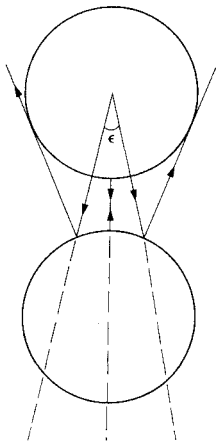

Fig. 2 Rays within the angle ϵ suffer multiple reflections and the rays beyond this are all reflected upward.

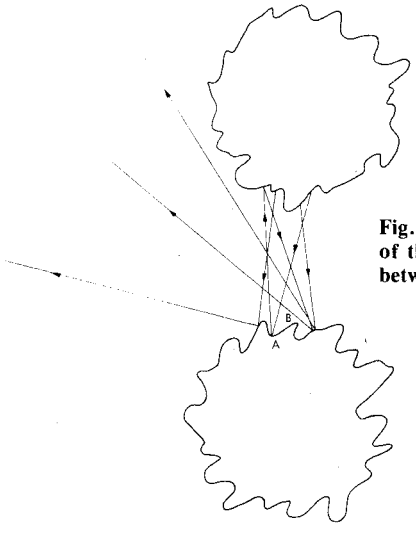

Fig. 3 Instantaneous picture of the jet boundaries and rays between the jets.

of the noise producing regions, which contribute to PNL, to the action of shielding. In this context it is observed that jets which are as close as 12% of their diameter exhibit shielding over all of the frequency band that can be shielded and, therefore, must have exposed all of the noise sources. High-speed jets spread less than low-speed jets; also, jets that discharge into a coflowing stream (e.g., in flight) spread less than jets that discharge into stationary surroundings. Thus there are additional favorable effects for shielding the noise of high-speed jets in flight for over/under-the-wing configurations.

The possibility of multiple reflections between the two jets is considered next. Figure 1 shows the time-averaged jet boundaries of two jets which merge at some point downstream. The rays of sound that undergo partial reflections are shown as dashed lines, and those that are totally reflected are solid lines. In the central plane, there is a question as to where a multiple-reflected ray finally ends. To consider this, the projection of rays has been drawn in a normal cross section in Fig. 2. In this figure, rays that are within the angle ϵ undergo multiple reflections, whereas, those that lie outside the angle ϵ are reflected upward. From such a time-average picture, however, it is not clear in which direction a ray finally leaves the jets. To help clarify this, Fig. 3 shows an instantaneous picture. An element AB of the lower jet takes many possible orientations of a fairly large slope with the time average being horizontal. This element can reflect the rays impinging on it over the upper half-space with approximately equal probability. The upper jet intercepts some of these rays and re-reflects them over the lower half-space, a small part of which is intercepted by the lower jet. It is clear that most of the rays are reflected upwards and some toward the ground, but none go through the lower jet. The sketch in Fig. 3 leads to the following simplification in the analysis: rays are traced through the lower jets and the transmission coefficients as they go through the various shear layers of the lower jet are calculated. The reflected waves at any interface are ignored because chances are that most of the energy of these is directed upward. In the case of total reflection, the ray is stopped at the first interface and no noise of the upper jet is heard on the ground at all. Naturally, the random reflections bring in the subject of scattering by turbulence. The following simple analysis shows that the scattering phenomenon is not important. The sound energy can be redistributed by scattering, which can therefore modify the directivity of a source without changing the total radiated power. An order-of-magnitude analysis of this effect is estimated as follows. G.I. Taylor[3] considered such dissipation of sound due to turbulence, where it is shown that the phase distortion of a plane wavefront which passes on through eddies of velocity amplitude u', is given by

$$\Delta\phi = kl\frac{u'}{C}\sqrt{n}$$

where l is the eddy length and k is the wave number of sound. In this process, the amplitude of the original wave of unit amplitude is reduced to $\cos\Delta\phi$ and the intensity correspondingly to $\cos^2\Delta\phi$.

An oblique ray from an upper jet can typically pass through nine eddies. If the diameter of the upper jet is about 1 m and a typical eddy size about a shear layer thickness, the axial location at which the sound ray encounters turbulence is about 0.3 m. Then, if a turbulence level in the eddy is taken to be

$$u'/c = 1/10$$

$$\Delta\phi = k(0.3)\frac{1}{10}\sqrt{9} = 0.09\,k$$

at a frequency of 100 Hz,

$$k = 2\pi(f/c) = 2\pi(100)/(350)$$

Therefore,

$$\Delta\phi = 0.09\times 2\pi\times(100/350)$$

$$= 18\pi/350$$

which is small compared to $\pi/2$. In this case, scattering is negligible; note, however, that the shielding is also small at this frequency because it is near the region of cutoff where the sound wavelength is proportional to jet circumference. If high frequencies, e.g., $f = 1000$ Hz, are considered, $\Delta\theta(18\pi/35)$, which is close to $\pi/2$. In this case, scattering is very strong. However, at this frequency, shielding is also strong and most of the sound does not penetrate the lower jet. Therefore, it appears that scattering is a minor correction to the small part of sound that does penetrate a jet.

III. Analysis

The intensity of noise emitted by a point source intercepted by a smooth slug flow jet will be derived in the following analysis.

The analysis has been developed so that PNLs on the ground plane can be calculated conveniently when an airplane is taking off. The jet axis is inclined at an angle with respect to the horizontal plane as shown in Fig. 4. The coordinates of any point P on the ground plane are X, Y, and Z referred to the origin S, which is at the midpoint of the exit plane of the two nozzles. The brake release point is designated as 0 and the axial coordinate based on 0 as the origin is X. Therefore,

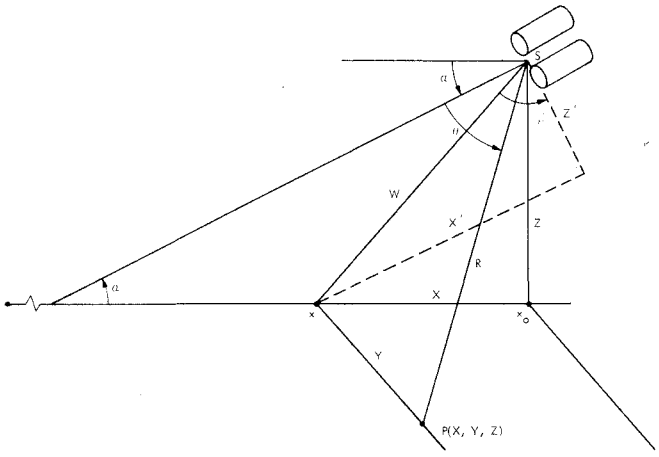

Fig. 4 Coordinate system for take-off drawn such that X, X', and β are negative.

$$X = x - x_0 \tag{1}$$

It is convenient to identify the location of point P by another system of coordinates shown in Fig. 4 as X', Y', and Z'. This new system of coordinates is prescribed such that X' is parallel to the bisector of the axes of the two jets. Then, from Fig. 4,

$$R = (X^2 + Y^2 + Z^2)^{1/2} \tag{2}$$

and

$$W = (X^2 + Z^2)^{1/2} \tag{3}$$

In terms of angles,

$$\beta = \alpha + \tan^{-1}(X/Z) \tag{4}$$

From these equations, the primed coordinates are obtained by using

$$Z' = W\cos\beta \tag{5}$$

$$X' = W\sin\beta \tag{6}$$

and

$$Y' = Y \tag{7}$$

A description of the acoustic shadow in the X', Y', Z' system of coordinates is obtained from the sketch in Fig. 5. The view factor H is defined as the ratio of the angle subtended by the "visible" part of the upper jet at P to the maximum angle of the upper jet $2\Delta\phi$. Thus,

$$H = [\phi_1 + \Delta\phi_1 - (\phi_2 + \Delta\phi_2)] \div 2\Delta\phi_1 \tag{8}$$

Now, if D denotes the diameter of each of the round jets which are separated by a distance S,

$$\phi_1 = \tan^{-1}\left[\frac{Z' + (D+S)/2}{Y'}\right] \tag{9}$$

$$\phi_2 = \tan^{-1}\left[\frac{Z' + (D+S)/2}{Y'}\right] \tag{10}$$

$$\Delta\phi_1 = \tan^{-1}[(D/2)/Y'\sec\phi_1] \tag{11}$$

$$\Delta\phi_2 = \tan^{-1}[(D/2)/Y'\sec\phi_2] \tag{12}$$

Thus H can be calculated by the use of Eqs. (8-12).

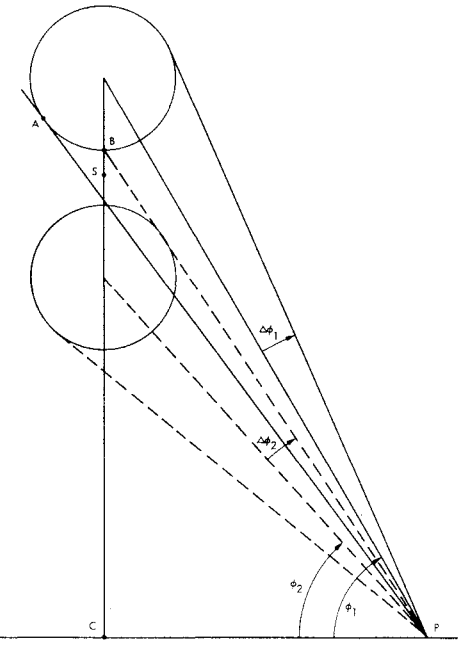

Fig. 5 Sketch for the evaluation of the shadow in the (Y', Z') plane showing the portions of the rays from A to B of the upper jet which are intercepted by the lower jet.

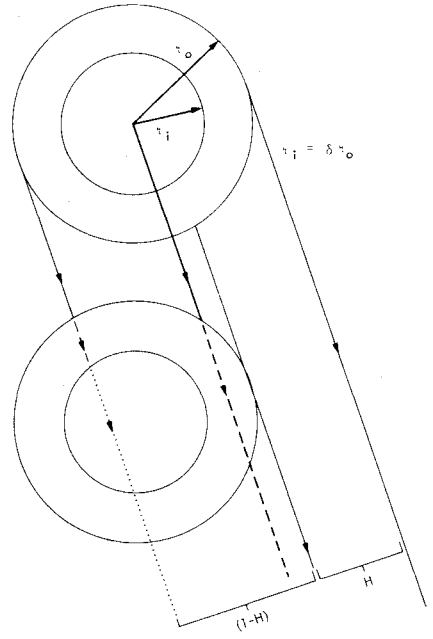

Fig. 6 View factors for directly radiated and refracted sound for coaxial jets each having inverted velocity profiles.

The portion of the sound radiated by the upper jet, which is transmitted unmodified, is proportional to the view factor H, whereas the remainder, which is proportional to the fraction $(1-H)$, undergoes refraction at the boundaries of the lower jet. Thus it is essential to characterize that which is refracted. To do this, let r_i and r_o be the inner and outer radii of the lower jet and define the quantity $\delta = r_i/r_o$. Figure 6 shows a sketch of the rays when the point of reception is far away so that the rays are essentially parallel near the jets. The part of the sound intercepted by the lower jet undergoes refraction at either two or four shear layer boundaries, depending on whether the sound is intercepted by the outer shear layer only or by both the outer and the inner shear layers of the lower jet. The transmission coefficients for these two cases are different and will be calculated using a two-dimensional model. The

fraction of the noise generated by the upper jet that crosses shear layer boundaries of the lower jet, and hence is refracted, are subdivided into portions which are proportional to geometric factors as follows:

1) The maximum which passes through the outer annulus is proportional to $(1-\delta)/2$.

2) The remainder of this, if there is any, passes through the core and is proportional to $[(1-H)-(1-\delta)/2]$.

3) The most that can pass through the core is proportional to δ.

4) If there is any remainder of this, it would be proportional to $[(1-H)-(1+\delta)/2]$ and would pass through the other side of the annulus only.

Next, let T_2 and T_4 represent the pressure transmission coefficients through two and four interfaces, respectively. It can then be seen that the mean-square pressure at the reception point is modified to the following expression:

$$\overline{p^2}\ \{H+[(1-\delta)/2]T_2^2+\delta T_4^2+[(1-H)-(1+\delta)/2]T_2^2\} \tag{13}$$

This expression applies for the case when $(1-H)>(1+\delta)/2$.

Refraction at a plane boundary was investigated by Ribner.[4] In the following example, a similar analysis for several boundaries is performed. As indicated in Fig. 7, the angle of incidence is given by

$$\epsilon=\tan^{-1}(-X'/Z') \tag{14}$$

This defines a Mach number M_s in the surroundings given by

$$M_s=1/\sin\epsilon \tag{15}$$

relative to the stationary ripple produced by the incident wave. The ripple velocity is given by

$$U=C_sM_s+U_s \tag{16}$$

where the subscript s refers to "surroundings." The Mach number in the region after the noise has passed through the first boundary (No. 1 in Fig. 7) is given by

$$M_o=(U-U_o)/C_o \tag{17}$$

where C_o is the speed of sound in the higher temperature outer flow identified by velocity U_o in Fig. 7. When $M_o<1$, there is

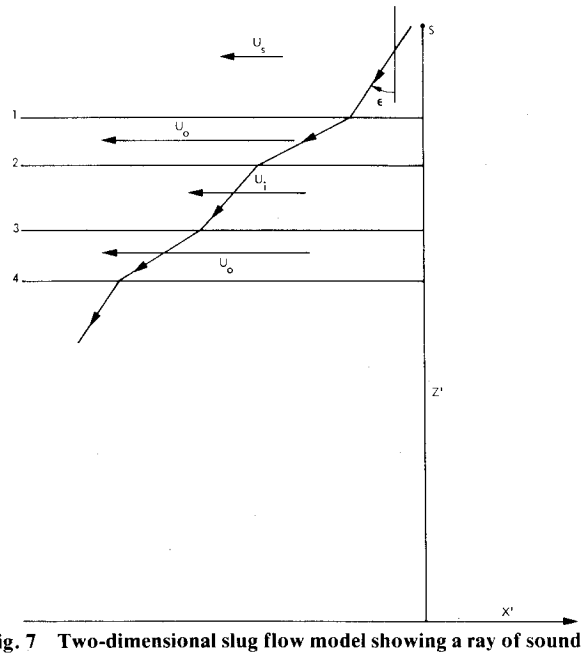

Fig. 7 Two-dimensional slug flow model showing a ray of sound.

total reflection at the interface and consequently no transmission through the jet occurs. In general, however, the pressure transmission coefficient can be shown to be

$$T_{so}=\frac{2}{1+Z_{so}} \tag{18}$$

The impedance Z_{so} is given by

$$Z_{so}=\frac{\rho_s(C_sM_s)^2\sqrt{M_o^2-1}\,\mathrm{sgn}M_o}{\rho_o(C_oM_o)^2\sqrt{M_s^2-1}\,\mathrm{sgn}M_s} \tag{19}$$

Between the first and second boundary, M_i is calculated by

$$M_i=\frac{U-U_i}{C_i} \tag{20}$$

For the sound that impinges on the second boundary, the impedance between o and i is given by

$$Z_{oi}=\frac{\rho_o(C_oM_o)^2\sqrt{M_i^2-1}\,\mathrm{sgn}M_i}{\rho_i(C_iM_i)^2\sqrt{M_o^2-1}\,\mathrm{sgn}M_o} \tag{21}$$

and the pressure transmission coefficient is

$$T_{oi}=\frac{2}{1+Z_{oi}} \tag{22}$$

At the next interface, Z changes to its reciprocal, i.e.,

$$T_{io}=\frac{2}{1+Z_{io}}=\frac{2}{1+(1/Z_{oi})} \tag{23}$$

and, finally, at the fourth boundary

$$T_{os}=\frac{2}{1+(1/Z_{so})} \tag{24}$$

The transmission of pressure is the product of all four or the product of the pairs $[T_{so}T_{os}]$ and $[T_{io}T_{oi}]$. Thus,

$$T_4=\frac{2Z_{so}}{(1+Z_{so})^2}\cdot\frac{2Z_{oi}}{(1+Z_{oi})^2}\ \text{and}\ T_2=\frac{2Z_{so}}{(1+Z_{so})^2} \tag{25}$$

The transmission of energy through the four interfaces is given by T_4^2. The ray of sound leaves the lower jet at the same angle as the angle of incidence. There is a large range of downstream angles for which the total reflection occurs from the first boundary. This condition, of course, results in good shielding of the noise radiated from the upper jet.

The shadow on the ground plane is of triangular shape, as shown in Fig. 8. In this figure, N and Q represent noisy and quiet jets, respectively. The two jets could, however, also radiate equal noise levels. J is the point at which the bisector of the engine axes intersects the ground plane. To the right of this point, the noise of the noisy jet is intercepted by the quiet jet, and in the shadow zone the noise levels are lower than to the left of J, where in that triangular segment the noisy jet intercepts the noise of the quiet jet. As the airplane climbs to higher altitudes, the shadow covers larger and larger areas, thereby reducing the noise over a greater area of the community.

The next step is to incorporate suitable expressions for the PNLs of jets having inverted velocity profiles. These are taken from Appendix B of Ref. 5.

For an engine producing a coaxial flow with velocity U_i in the core and a velocity U_o in the outer annulus, the total mass

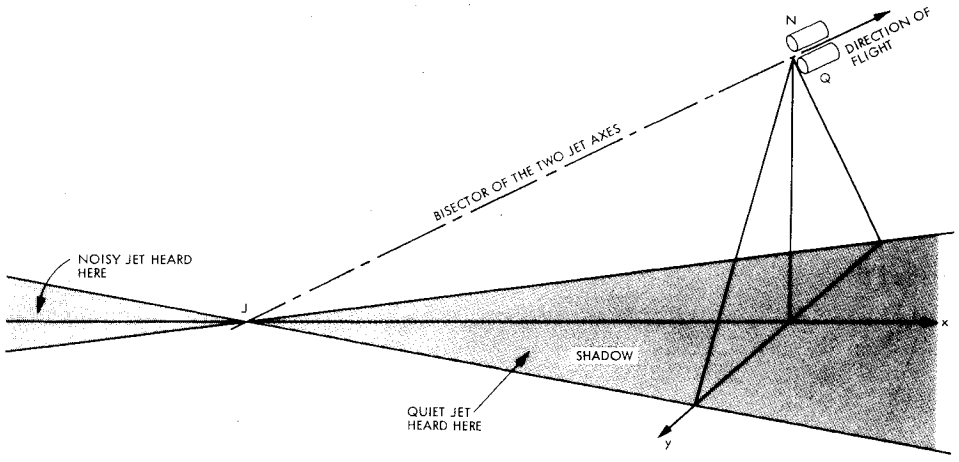

Fig. 8 Shape of the shadow in the ground plane.

flux is given by

$$\dot{m}_T = \pi r_i^2 \rho_i U_i + \pi (r_o^2 - r_i^2) \rho_o U_o \tag{26}$$

This produces a jet thrust

$$F = \pi r_i^2 \rho_i^2 U_i^2 + \pi (r_o^2 - r_i^2) \rho_o U_o^2 \tag{27}$$

The mixed mean velocity V_{mix} and the mixed mean density ρ_{mix} are defined by

$$V_{\text{mix}} = (F/\dot{m}_T) \tag{28}$$

$$\rho_{\text{mix}} = (\dot{m}_T/\pi r_o^2 V_{\text{mix}}) = (F/\pi r_o^2 V_{\text{mix}}^2) \tag{29}$$

The maximum perceived noise level (PNL_{max}) at a 731.5 m (2400 ft) sideline distance is given by

$$\begin{aligned}\text{PNL}_{\text{max}} &= 78.1 + 1.5 - 1.59 \log [(r_o/r_i)^2 - 1] \\ &- 22.9 \log (r_o/r_i) + 10 \log (F/5130) + 20 \log (\rho_{\text{mix}}/\rho_s) \\ &+ 80.3 \log (V_{\text{mix}}/C_s) - 25 \log (R \sin\Theta_i/731.5) + (\Delta\text{PNL})_f\end{aligned} \tag{30}$$

In Eq. (30), ρ_s and C_s represent the density and the speed of sound in the surroundings, respectively. The constant 1.5 represents the increase due to ground reflections. The inverse-square law has been modified to

$$-25 \log (R \sin\Theta_i/731.5)$$

instead of

$$-20 \log (R \sin\Theta_i/731.5)$$

as indicated in the previously stated document on General Electric engines. The angle to the inlet is

$$\Theta_i = 180 - \Theta \tag{31}$$

The quantity $(\Delta\text{PNL})_f$ is the modification due to the effect of flight and is given by

$$\begin{aligned}(\Delta\text{PNL})_f &= 10\, b \log [V_{\text{mix}}/(V_{\text{mix}} - U_s)] \\ &+ 10 \log [1 - (U_s/C_s) \cos\Theta_i]\end{aligned} \tag{32}$$

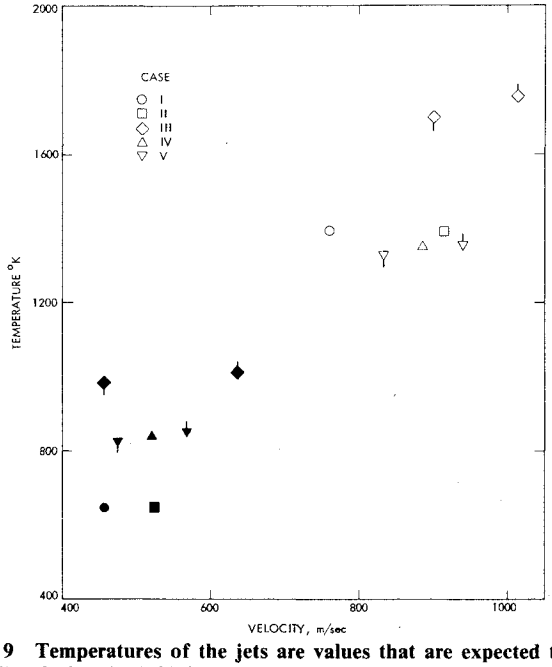

Fig. 9 Temperatures of the jets are values that are expected to be possible during the 1980-85 time period. The solid symbols correspond to the lower temperature core flow and the open symbols refer to the annular flow. A tic below a symbol refers to the lower engine and a tic above refers to the upper engine.

The quantity b is given by

$$b = 3.49 + 5.52[(\Theta_i - 130)/40] + 2.10[(\Theta_i - 130)/40]^2 \tag{33}$$

The flight exponent b is probably sensitive to the mixture of jet noise and core noise and may be modified when data on variable cycle engines become available. The angular distribution of PNL on the sideline is given by

$$\begin{aligned}\text{PNL} &= \text{PNL}_{\text{max}} - 7.5 && \text{for } 0 \le \Theta_i < 107 \\ &= \text{PNL}_{\text{max}} - 0.23(140 - \Theta_i) && \text{for } 107 \le \Theta_i < 140 \\ &= \text{PNL}_{\text{max}} - 0.36(\Theta_i - 140) && \text{for } 140 \le \Theta_i < 150 \\ &= \text{PNL}_{\text{max}} - 1.14(\Theta_i - 146.8) && \text{for } 150 \le \Theta_i < 160 \\ &= \text{PNL}_{\text{max}} - [3.36 - 25 \log \sin\Theta_i + 0.32(\Theta_i - 160)] \\ & && \text{for } 160 \le \Theta_i < 180\end{aligned} \tag{34}$$

The last equation for $160 \leq \Theta_j < 180$ has been written in order to produce a drop of 0.32 dB/deg at a fixed distance from the source. This is the rate of fall of the overall sound pressure level (OASPL) exhibited by pure jet noise at a jet velocity equal to twice the ambient speed of sound.[6]

The sound pressure of the two jets is obtained by mean square addition.

$$(\mathrm{PNL}) = 10\log\left\{10^{(\mathrm{PNL})_{far}/10}\left[H+\frac{(1-\delta)}{2}T_2^2+T_4^2 + \left[1-H-\frac{(1+\delta)}{2}\right]T_2^2\right]+10^{(\mathrm{PNL})_{near}/10}\right\} \quad (35)$$

where $(\mathrm{PNL})_{far}$ and $(\mathrm{PNL})_{near}$ refer to the perceived noise levels of the far and near jets when they occur alone.

IV. Results and Discussion

In all cases, the jet velocity profile was assumed to be inverted. The flight trajectory that was used in all of these calculations is tabulated in Ref. 7. The airplane lifts off at 48 s from brake release and α changes to approximately 16 deg and remains constant during the climb. The velocity of the airplane remains nearly constant at about 107 m/s during climb. At 83 s from start, the airplane is over the 3.5 n. mi. location at a height of 388 m.

This flight path is for a supersonic airplane which has a gross weight of 333,260 kg and a wing loading W/S of 4190 N/m^2. The thrust-to-weight (T/W) ratio is 0.28. The conditions for all of these cases are given in Fig. 9. It is assumed that the engine size for all cases is the same as for the P&WA VSCE 516, i.e., the core area is 0.64 m^2 and the bypass area is 0.96 m^2. The total static thrust of the engines for the various cases are different. To keep the flight path the same, values of thrust were held constant by appropriately reducing engine sizes. In this procedure, the noise levels change as 10 log (F/F_{ref}) or as 10 log [area/(area)$_{ref}$]. This reduction in engine size to decrease thrust is very inefficient for noise suppression. The noise correction levels ΔdB are -0.2, -2.1, -1.0, 0, 0 for cases I-V. These ΔdB values were added to the PNL values calculated for the various cases.

The various cases considered are summarized as follows:

Case no.

I — Equal engine parameters for the upper and lower engines. The engines are somewhat smaller than those in cases IV and V in order to reduce thrust from 1.12-1.07 MN (250,000-240,000 lb).

II — Equal engine parameters for the upper and lower engines, but of higher velocities than in case I. The engine size was reduced more than for case I.

III — Unequal upper and lower engine flow conditions, but of higher exhaust temperature than cases I and II. Also, the engine size is smaller than for cases IV and V.

IV — Equal engine parameters corresponding to the P&WA VSCE 516 powerplant.

V — Unequal upper and lower engine parameters representing cutback of the thrust of the lower engine. The engines are the same as in case IV.

The flow conditions are shown graphically in Fig. 9.

The contours of PNL on the ground plane, which include the contours in the shadow zone (i.e., noise reduction when compared to an engine side-by-side arrangement), are shown in Figs. 10 and 11 for case V-B. The letter "B" indicates a spacing between the engine axes equal to 1.2 times the exit diameter of one engine. Even at a closer spacing of 1.1 times the exit diameter of one engine, the data shown in Ref. 1 exhibit very good shielding. The contours in Figs. 10 and 11 show the typical butterfly shape for jet noise and the triangular shape for the shadow. The figure titles describe the

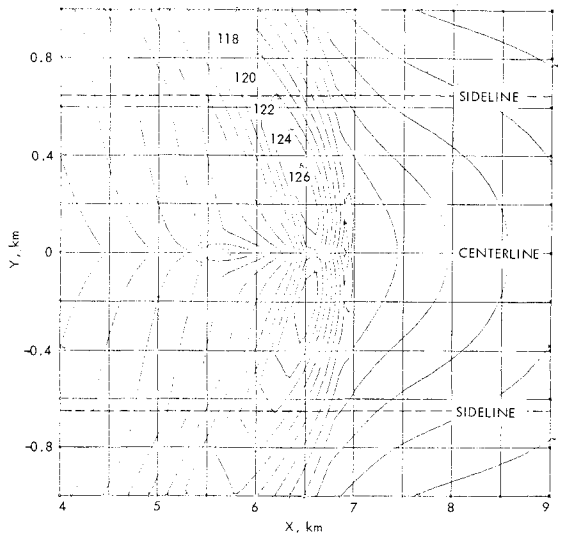

Fig. 10 Case V-B: X and Y are in km; the airplane is at $X = 6.92$ km at a height $H = 435$ m; contour D is 122 PNdB and the interval between contours is 2 PNdB. At $X = 3.5$ n. mi., i.e., $X = 6.5$ km, the noise level is 120 PNdB.

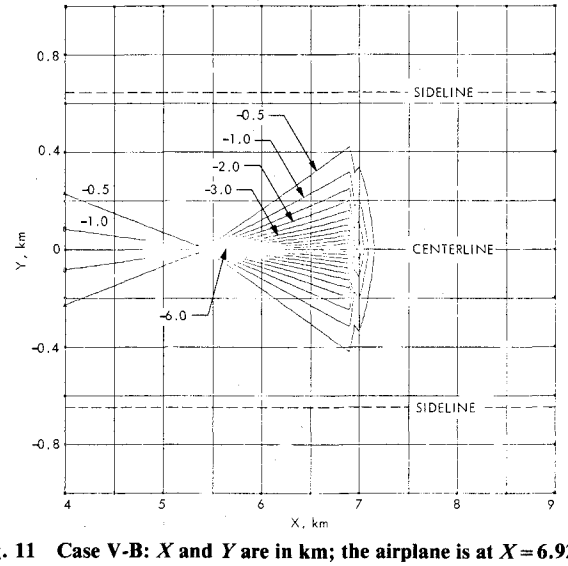

Fig. 11 Case V-B: X and Y are in km; the airplane is at $X = 6.92$ km at a height $H = 435$ m; the shadow does not reach to the 650 m sideline but offers a noise reduction of 6 dB at 6.5 km on the centerline; contour A is $-1/2$ dB and decreases at 1/2 dB intervals.

manner in which the noise levels vary as the airplane flies by. The maximum noise reduction on the centerline was found to be 6 PNdB. However, at a sideline distance of 650 m, there was no noise reduction due to shielding.

The time histories of relative PNL values are shown in Fig. 12 for case III-B. The figure titles include the changes in EPNL values and for ease of comparison these values are listed in Table 1.

In all cases, the shielded EPNL values at the centerline on the ground at a location of 3.5 n. mi. from brake release are close to the noise levels that exist at 0.35 n. mi. at the sideline at the same distance from the brake release point. In case III-B, the sideline noise is about 2 dB higher. Extra ground attenuation of about 4 EPNdB has been observed in flight tests of the Concorde airplane[5] and, if this reduction is assumed to be the same for the present cases, the dominant noise levels will be the flyover levels. The lowest noise levels for the five cases considered are for case I-B. The reason for this is that the engines were taken to operate at lower velocities and temperatures at the same total thrust.

Table 1 Effective perceived noise levels on the ground plane at $x = 3.5$ n. mi. from brake release

Case no.	I – B	II-B	III-B (unsymmetric)	IV-B	V-B (unsymmetric)
Centerline ($Y = 0$) side-by-side engine configuration (for reference)	107.7	123.9	123.4	120.7	121.2
Centerline over/under engine configuration	114.7	120.9	117.7	117.7	116.3
Change in noise on centerline due to shielding	−3.0	−3.0	−5.7	−3.0	−4.9
Sideline over/under configuration at $X = 3.5$ n. mi $Y = 0.35$ n. mi	114.2	120.3	119.5	117.0	117.5

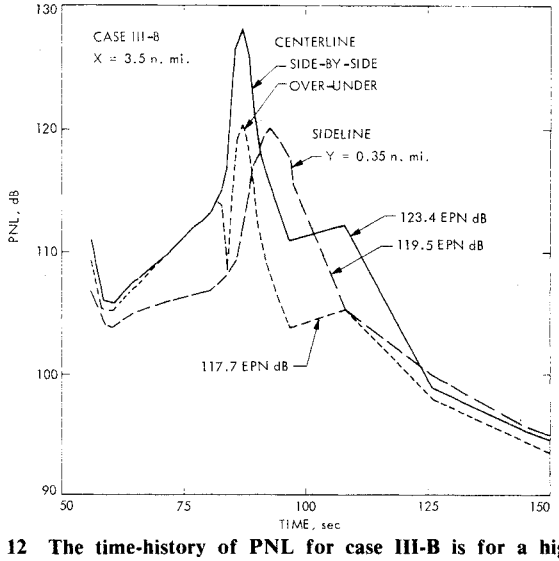

Fig. 12 The time-history of PNL for case III-B is for a higher velocity, smaller size engine. On the centerline, shielding reduces the EPNL from 123.4 to 117.7 EPNdB, i.e., by 5.7 EPNdB. The sideline noise uncorrected for ground attenuation is 119.5 EPNdB, and with a 4 dB ground attenuation reaches 115.5 EPNdB, which is smaller than the centerline noise level of 117.7 EPNdB.

By comparing the symmetric case I-B with an unsymmetric one, e.g., III-B, it is apparent in Table 1 that an symmetric one, e.g., III-B, it is apparent in Table 1 that an additional 2.7 dB reduction could be achieved by making the engine parameters of case I-B unsymmetrical. With this potential reduction in PNL, a flyby noise level of 111.0 EPNdB and a sideline noise of 110.2 EPNdB could be attained. A 4dB ground attenuation was incorporated in the sideline value. Even more asymmetry in the engine parameters might be possible in practice.

Recent experimental data of the flight of F15 which has two engines close by are presented by Clauss et al.[8] for the cases of equal thrust and also differential thrusts on the two engines. In Fig. 19 of Ref. 8, shielding benefits of 3dB for the symmetric case and values between 4 and 5dB for the unsymmetric case are observed. These compare favorably with the values in the third row of Table 1.

V. Directivity of Noise Radiated from Four Engines

The analysis performed thus far is applicable to one jet which shields only one other jet. Thus a brief examination of shadows formed by each jet noise source of the remaining three jet flows will be carried out so that comparisons can be made for the configuration of four engines in-line under-the-wing with the two-over/two-under engine configuration.

The four-in-line configuration with equal thrust from each engine is considered first. For this case there is no shadow directly under the airplane. The noise level radiated directly under the airplane by this arrangement is taken as the reference value for all comparisons and is set equal to 0 dB. At 90 deg to the vertical, the shadow for the in-line case is the strongest (results in the lowest noise level below the reference) and only the noise source nearest the observer is heard. Therefore, the intensity at $\phi = 90$ deg is one-quarter the total intensity, i.e., there is a 10 log 4 or 6 dB reduction at this location. Values of noise reduction when many shadows are superposed can be easily obtained. Sketches of such shadows are shown in Ref. 7. At an angle $\phi \approx 60$ deg, the noise reduction is negligible. This is the region at the sideline where the noise measurement station is located in conformity with the present noise regulations to evaluate the noise level of an airplane taking off along a typical trajectory.

Additional shadows result in the two-over/two-under configuration. The shadows are extensive and significantly benefit the community directly under the aircraft. If the thrust of the upper engines are 16% above normal and those of the lower engines are 16% below normal, the total thrust is the same as before, but because only the quieter engines are heard directly under the aircraft, a 6 dB reduction is achieved. If the spanwise separation between the two engine pairs is large, there will be no shadow at $\phi \approx 60$ deg. If the engines were spaced more closely in the spanwise direction, this gap in which no noise reduction is shown could be eliminated. In all of these comparisons of the shadows, energy was conserved; hence, the sound that does not reach the shadow zones is redirected. For the over/under configurations, for example, noise produced by the upper engines is largely reflected upward and is not heard by the community below. Some of the noise is also scattered sideways, and in the previous analysis, it was shown that the increase in values of PNL that results from scattering is small.

VI. Summary and Conclusions

A simple model has been developed for the calculation of perceived noise levels and noise reduction at takeoff for an airplane using engines in the over/under-the-wing configurations. All noise reductions are referred to the case of engines located in-line under the wing. The analysis was conducted for a four-engine airplane with the two over/under engine pairs separated by a somewhat larger spanwise distance than might be used in an actual aircraft. Closer spacing of the engines would result in wider shadow zones and additional shadows and hence, would improve noise reduction over a wider area. For example, for the case

analyzed, there is a sideline region not covered by the shadow; however, this could be overcome by spacing the engines closer together. When the spanwise separation between the right and left engines is large, the analysis can be performed with a single pair of over/under engines and the sound intensities can then be doubled. This approach was used in the present analysis.

In the over/under engine arrangement, the noise of the upper engine is partially reflected upward by the lower jet flow which results in lower noise levels on the ground plane. A beneficial noise reduction is always observed, and when the thrust of the lower engine is reduced and the thrust of the upper engine is increased, keeping the total thrust constant, noise reduction up to about 6 PNdB is observed under the aircraft. At a measuring station of 3.5 n. mi. from the brake release point, an effective noise reduction of as much as 6 EPNdB can be obtained.

Time histories of relative perceived noise levels for several cases were obtained corresponding to jet flow temperatures generated by engines incorporating material technology of the 1980-85 time period. For the over/under engine configuration, jet shielding at a sideline distance of 0.35 n. mi. (at an angle with respect to horizontal of about 25 deg) is negligible. In all of the cases considered with a particular takeoff trajectory, supersonic inverted velocity profile jets were assumed. It was found that community noise levels for a four-in-line engine configuration under the wing are larger than the EPN values at the sideline. However, the shielding offered by the over/under concept reduces the flyover noise levels to approximately those of the sideline values. Because extra ground attenuation reduces the sideline noise further by typically 4 EPNdB, the noise under the aircraft is still the dominant one, even with the amount of asymmetry considered in the thrust levels of the upper and lower engines. Results of the present studies indicate that FAR 36 (1969) regulations barely can be met by a supersonic cruise vehicle using the variable cycle engines and readjustment of the thrust without cutback and without the use of a mechanical suppressor. Further detailed studies incorporating larger reduction of thrust on the lower engines with corresponding trajectory modifications would be necessary to optimize the design. In these studies, two engines over the wing and two engines below could be studied to examine the benefits of all the shadows that arise. Scattering, which was shown to be of small importance, could also be modeled to give better predictions in the upstream quadrant where jet noise is low.

Acknowledgment

Research described in this paper was carried out at the Jet Propulsion Laboratory, California Institute of Technology and was sponsored by Lockheed California Company through an agreement with NASA.

References

[1] Bhat, W.V., "Experimental Investigation of Noise Reduction from Two Parallel-Flow Jets," *AIAA Journal,* Vol. 16, Nov. 1978, pp. 1160-1167.

[2] Kantola, R.A., "Shielding Aspects of Heated Twin Jet Noise," AIAA Paper 77-1288, presented at the AIAA 4th Aeroacoustics Conference, Atlanta, Ga., Oct. 3-5, 1977.

[3] Taylor, G.I., "The Scientific Papers of Sir Geoffrey Ingram Taylor," Vol. II, edited by G.K. Batchelor, Cambridge, 1960, pp. 33-35.

[4] Ribner, H.S., "Reflection, Transmission, and Amplification of Sound by a Moving Medium," *Journal of the Acoustical Society of America,* Vol. 29, April 1957, pp. 435-441.

[5] "Supersonic Cruise Vehicle Assessment Study of an Over/Under Engine Concept" dealing with "General Electric Engines" prepared under Contract No. NASI-14625, Lockheed-California Company for NASA Langley Research Center, Hampton, Va., Oct. 1977.

[6] SAE Aerospace Recommended Practice, ARP 876.

[7] Parthasarathy, S.P., Cuffel, R.F., and Massier, P.F., "Twin Jet Shielding," AIAA Paper 79-0671 presented at the AIAA 5th Aeroacoustics Conference, Seattle, Wash., March 12-14, 1979.

[8] Clauss Jr., J.S., Wright, B.R., and Bowie, G.E., "Twin Jet Shielding for a Supersonic Transport" presented as Paper 79-0670 at the AIAA 5th Aeroacoustics Conference, Seattle, Wash., March 12-14, 1979; also *Journal of Aircraft,* Vol. 17, Aug. 1980.